Applied Mathematics & Information Sciences
An International Journal

http://dx.doi.org/10.12785/amis/081L29

Design and Implementation of Optimal Fuzzy PID Controller for DC Servo Motor

Her-Terng Yau[1,*], *Po-Hsien Yu*[2] *and Yuan-Hung Su*[3]

[1] Department of Electrical Engineering, National Chin-Yi University of Technology, Taichung, Taiwan
[2] Department of Mechanical and Electro-Mechanical Engineering, National Sun Yat- Sen University, Kaohsiung, Taiwan
[3] Department of Electrical Engineering, Far-East University, Tainan, Taiwan

Received: 5 May. 2013, Revised: 30 Aug. 2013, Accepted: 31 Aug. 2013
Published online: 1 Apr. 2014

Abstract: A method is proposed for improving the transient positioning response of a DC servo motor controlled by a proportional-integral-derivative (PID) controller. In the proposed approach, the optimal gains of the PID controller are determined using an Evolutionary Programming (EP) scheme and a Genetic Algorithm (GA), respectively, based on an integrated-absolute error (IAE) fitness function. The optimal gain constants obtained using the two methods are then fine tuned using a Fuzzy Logic Controller (FLC). The experimental results show that the FLC controller yields an effective improvement in the positioning response of the DC servo motor compared to that obtained using the optimized PID controller alone. In addition, it is shown that the FLC + EP based PID controller provides a more rapid response than the FLC + GA based PID controller. The effectiveness of proposed controllers is verified experimentally.

Keywords: Evolutionary Programming; Genetic Algorithm; DC servo motor; PID controller; Fuzzy Logic Controller

1 Introduction

DC motors have a simple structure, a small size, physical robustness, and high reliability. As a result, they are used in many industrial and commercial applications, including automated production, precision turntable devices, electric wheel chairs, elevators, electric bicycles, electric scooters, and so on. However, the performance of DC motors is reliant on the use of highly-precise control schemes. Of the various control methods available, DC motors in the industrial domain are most commonly controlled using some form of proportional-integral-derivative (PID) system on account of their simple structure, straightforward implementation and low maintenance requirements. However, the performance of PID controllers relies in turn on an appropriate optimization of the PID parameters (i.e., the gain constants).

The literature contains many heuristic methods for solving optimization and search-type problems. Typical examples include Genetic Algorithms (GAs) (Lin & George Lee, 1996), Evolutionary Algorithms (EAs) (Fogel, 1999) and Evolutionary Programming (EP) (Hung, Lin, Yan & Liao, 2008). Notably, all of these methods are based on techniques inspired by the natural evolution process, such as mutation, selection and crossover. However, in the control field, the optimal system performance is generally achieved using standalone FLC (Fuzzy Logic Controller) or SMC (Sliding Mode Controller) schemes [1,2,3,4].

In [5], the authors proposed a simple adaptive observer for estimating the load torque and optimal control parameters of a typical commercial DC servo motor. Meanwhile, the authors in [6] presented a fuzzy-PID control scheme with inherent optimal-tuning features for both optimizing the local performance of a DC servo motor and improving its global tracking robustness.

The present study proposes two optimized PID-based control schemes for improving the transient positioning response of a DC servo motor. In the proposed approach, the optimal gains of the PID controller are determined using an EP algorithm and a GA, respectively, based on an integrated-absolute error (IAE) fitness function. The optimal gains obtained using the two algorithms are then further tuned using a FLC scheme. The performance of

* Corresponding author e-mail: htyau@ncut.edu.tw, pan1012@ms52.hinet.net

the two control methods is evaluated experimentally using a commercial DC servo motor.

The remainder of this paper is organized as follows. Section 2 briefly reviews the structure and theoretical background of DC servo motors. Section 3 introduces the EP and GA optimization methods and describes the basic principles of the FLC control scheme. Section 4 describes the hardware and system architecture employed in the experimental stage of the study. Section 5 presents the experimental results. Finally, Section 6 provides some brief concluding remarks.

2 DC Servo Motor

Figure 2.1 illustrates the basic structure of a DC motor. Note that the various annotations in the figure are defined as follows:

V_m : Armature circuit voltage
I_m : Armature circuit current
R_m : Armature resistance
L_m : Armature inductance
E_{emf} : Motor back-emf voltage
θ_m : Motor shaft position
T_m : Torque generated by motor

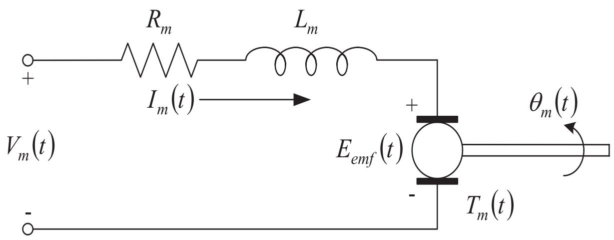

Figure 2.1: Basic structure of DC motor.

From Kirchhoff's voltage law, the armature voltage is given as

$$V_m - R_m I_m - L_m \frac{dI_m}{dt} - E_{emf} = 0 \tag{2.1}$$

Since $L_m \ll R_m$ for a typical DC servo motor, the motor inductance can be ignored. Therefore, from Eq. (2.1), the armature circuit current is obtained as

$$I_m = \frac{V_m - E_e m f}{R_m} \tag{2.2}$$

Furthermore, since the motor back-emf voltage $E_e m f$ and motor shaft angular velocity ω_m are directly related, the armature circuit current can be further expressed as

$$I_m = \frac{V_m - K_m \omega_m}{R_m} \tag{2.3}$$

where K_m is the back-emf voltage constant. From Newton's Second Theorem, the equilibrium load acting on the motor can be obtained as

$$J_m \dot{\omega}_m = T_m - \frac{T_l}{\eta_g K_g} \tag{2.4}$$

$\frac{T_l}{\eta_g K_g}$ is the load torque seen through the gears. (Note that η_g is the transmission efficiency of the gears.) Meanwhile, observed from the load of the motor, and applying Newton's Second Theorem once again, the following load balance is obtained:

$$J_l \dot{\omega}_l = T_l - B_{eq} \omega_l \tag{2.5}$$

where T_l represents the load and B_{eq} is the viscous damping coefficient as seen at the output. Substituting Eq. (2.4) into Eq. (2.5), yields the following:

$$J_l \dot{\omega}_l = \eta_g K_g T_m - \eta_g K_g J_m \dot{\omega}_m - B_{eq} \omega_l \tag{2.6}$$

Since $\omega_m = K_g \omega_l$ and $T_m = \eta_m K_t I_m$, Eq. (2.6) can be rewritten as

$$J_l \dot{\omega}_l + \eta_g K_g^2 J_m \dot{\omega}_l + B_{eq} \omega_l = \eta_g \eta_m K_g K_t I_m \tag{2.7}$$

Substituting Eq. (2.3) into Eq. (2.7) and taking the Laplace transform, the following transfer function between the armature voltage and the DC motor speed is obtained:

$$\frac{\omega_l(s)}{V_m(s)} = \frac{\eta_g \eta_m K_t K_g}{J_{eq} R_m s + B_{eq} R_m + \eta_g \eta_m K_m K_t K_g^2} \tag{2.8}$$

where $J_{eq} = J_l + \eta_g J_m K_g^2$. Since the position of the DC motor is given by the integral of the motor speed, the transfer function between the armature voltage and the DC motor position can be obtained as

$$\frac{\theta_l(s)}{V_m(s)} = \frac{\eta_g \eta_m K_t K_g}{s(J_{eq} R_m s + B_{eq} R_m + \eta_g \eta_m K_m K_t K_g^2)} \tag{2.9}$$

where θ_l is the position of the DC motor. Substituting the parameters of the DC motor used in the experimental stage of this study (i.e., SRV02, Quanser Inc.) into Eq. (2.9), the following transfer function is obtained:

$$\frac{\theta_l(s)}{V_m(s)} = \frac{0.33398}{s(0.00542s + 0.18989)} \tag{2.10}$$

In general, the PID controller used to control the DC servo motor can be defined as follows:

$$u(t) = K_p + K_d \frac{de(t)}{dt} + K_i \int_0^t e(\tau) d\tau$$

where K_p is the proportional gain, K_d is the differential gain, and K_i is the integral gain.

3 EP and GA Optimization Methods and FLC Control Scheme

3.1 Evolution Programming

Evolutionary programming (EP) was first proposed by Fogel [1] as an approach for achieving artificial intelligence. As shown in Fig. 3.1 and discussed below, EP comprises five main steps.

1) Population: Generate an initial population of candidate solutions $g_0 = [g_1, g_2, \cdots, g_N]$ of size N by randomly initializing each candidate solution vector $g_i \in S$, $i = 1, 2, \cdots, N$ in accordance with a quasi-random sequence (QRS).

2) Fitness scaling: Determine the quality of each candidate solution using a performance metric such as the integrated-absolute error (IAE) function, i.e.,

$$IAE = f_i = \int_0^\infty |e(\tau)| d\tau \tag{3.1}$$

where $e(\tau)$ is the error between the input and output.

3) Mutation: Mutate every $i = 1, 2, \cdots, N$, basing on the statistics, to double the population size from N to 2*N. Thereafter, generate a new population of candidate solutions g_{i+N} by means of the following equation:

$$g_{i+N,j} = g_{i,j} + N(0, \beta \frac{f_i}{f_\Sigma}) \ , \ \forall j = 1, 2, 3 \tag{3.2}$$

where $g_{i,j}$ denotes the jth element of the ith individual; $N(0, \beta \frac{f_i}{f_\Sigma})$ represents a Guassian random variable with zero mean and a variance of $\beta \frac{f_i}{f_\Sigma}$,; f_Σ is the sum of all the fitness scores; and β is a scale parameter with the form $\frac{f_i}{f_\Sigma}$.

4) Competition: Calculate the fitness score f_{i+N} for every g_{i+N}, $i = 1, 2, \cdots, N$, using Eq. (3.1). Perform a stochastic competition process in which g_i, $i = 1, 2, \cdots, N$ randomly competes with g_j, $j = 1 + N, \cdots, 2N$. If $f_i < f_j$, then declare g_i as the winner; otherwise, declare g_j as the winner and replace g_i with g_j. Following the competition process, choose N winners for the next generation and select the individual with the minimum objective function (i.e., the minimal value of Eq. (3.1)) among all the N winners as g_1.

5) Termination criteria: If the value of f_Σ converges to a minimum value, then select $g^* = g_1$ as the global optimum value; otherwise return to Step 3 (Mutation).

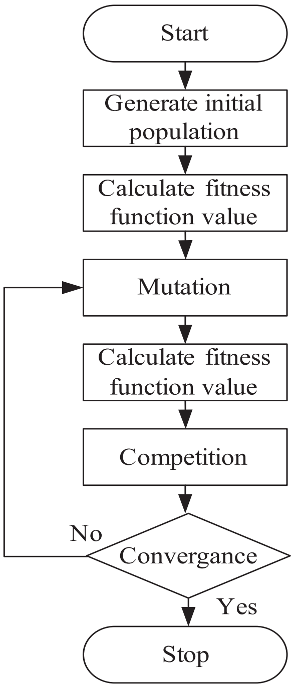

Figure 3.1: Flow chart of EP optimization procedure.

3.2 Genetic Algorithm

Figure 3.2 illustrates the basic steps in the Genetic Algorithm (GA) solution procedure. As shown, the procedure commences by establishing an initial population of candidate solutions. During each successive generation, a proportion of the existing population is selected and then subjected to crossover and mutation operations in order to generate new candidate solutions with a higher quality. The quality of the generated offspring are evaluated using a fitness function and the population is then updated accordingly. The process of selection, crossover and mutation is repeated iteratively until the predefined termination criteria are satisfied (typically, a certain number of iterations have been performed, or the error between the optimal solution and the best solution in the current generation falls within a pre-specified error range or remains unchanged for a certain number of iterations).

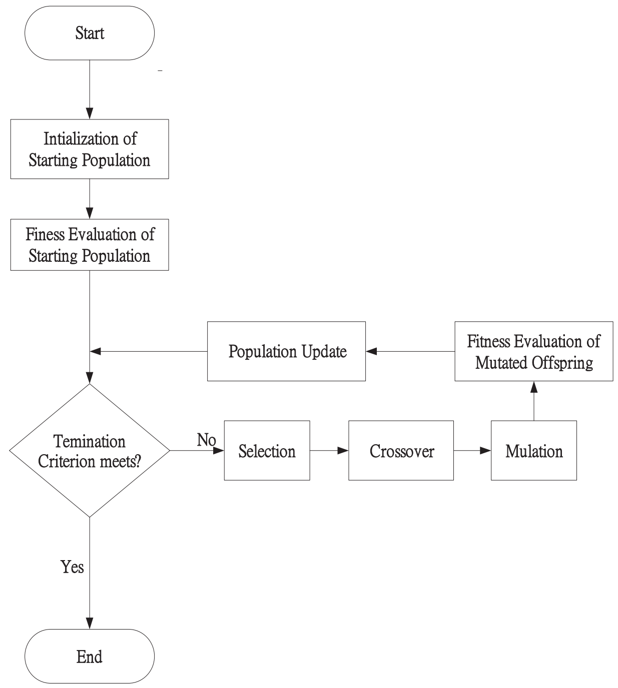

Figure 3.2: Flow chart of GA optimization procedure.

3.3 *Fuzzy Logic Controller*

As shown in Fig. 3.3, a Fuzzy Logic Controller (FLC) comprises five main function blocks, namely:

1) A rule base containing a number of fuzzy if-then rules expressed in the form ”If *a* is *A* then *b* is *B*”, where *a* and *b* are linguistic variables, and *A* and *B* are linguistic values characterized by membership functions.

2) A database defining the membership functions of the fuzzy sets used in the fuzzy rules.

3) A decision-making unit to perform inference operations based on the fuzzy if-then rules.

4) A fuzzification interface to transform the crisp inputs into corresponding fuzzy values.

5) A defuzzification interface to transform the fuzzy inference results into a crisp output.

In practice, various deuzzification schemes are available, including MC, MOM, COA and WAM [3]. In the present study, the defuzzification process is performed using the WAM method, i.e.,

$$y^{*}=\frac{\sum_{i}\max_{k}\mu_{C_k}(y_i)y_i}{\sum_{i}\max_{k}\mu_{C_k}(y_i)} \qquad (3.3)$$

where $\mu_{C_k}(y_i)$ is the membership function; y_i is the crisp output of the ith fuzzy rule ; and y^* is the output.

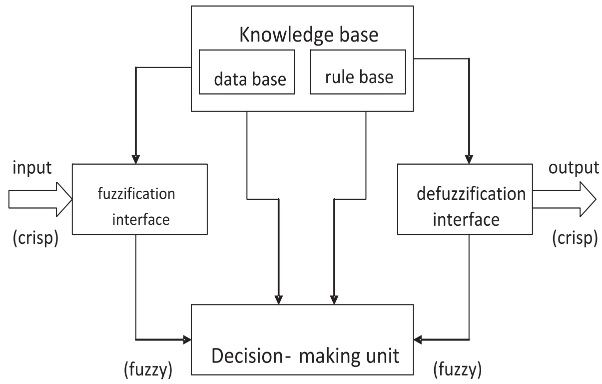

Figure 3.3: Configuration of fuzzy logic controller.

4 Hardware Architecture

In the present study, two different PID-based control schemes were developed for the DC servo motor, namely FLC + EP and FLC + GA. The optimal gains of the two control schemes were determined via MALAB / SIMULINK simulations. The performance of the two schemes was then evaluated using the experimental setup shown in Fig. 4.1 given an instructed shaft rotation of 45°. In the experimental tests, the control signal generated by each controller was interfaced from the computer to a D/A card and the resulting analog signal was then transmitted to the servo motor. The rotational position of the servo motor shaft was detected using a position sensor and transferred to an A/D card. The resulting digital output was then interfaced to the PID controller as a feedback signal. Having computed the positioning error, the PID controller issued a new control signal to drive the motor shaft toward the desired position. The control / feedback process was repeated iteratively until the positioning error converged to zero. The main items of hardware in the experimental setup are described in the sections below.

4.1 *DC motor*

The present experiments were performed using an SRV02 servo motor (Quanser Inc. [7]). The device consisted of a DC motor in a solid aluminum frame. The motor was equipped with a gearbox used to drive an external set of gears. Moreover, the motor was fitted with a potentiometer to measure the rotational position of the output shaft.

4.2 *Power amplifier*

The servo motor was driven by a Universal Power Module (UPM1503) consisting of a ±12 V power supply, analog sensor inputs and a power-amplified analog output. Note that the UPM ports were used to provide test points in addition to the standard connections in order to provide complete access to the inherent signals.

4.3 D/A and A/D adapters

The control signal issued from the PID controller to the servo motor was interfaced through a D/A card, while the position feedback signal from the motor was interfaced to the controller through a A/D card.

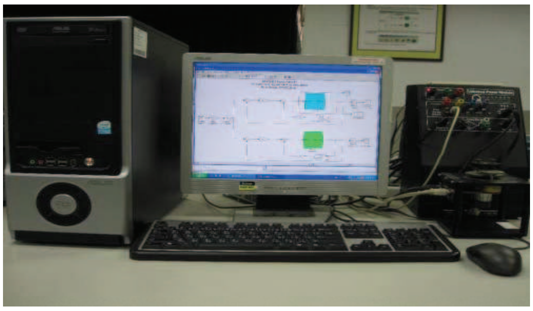

Figure 4.1: Photograph of experimental setup.

5 Results and Discussion

Figures 5.1 and 5.2 illustrate the basic structures of the EP(GA)-based PID controllers and FLC+EP(FLC+GA)-based PID controllers, respectively. In implementing the EP and GA optimization algorithms, the candidate solutions were expressed in the form of three-element vectors $[\ K_p \quad K_i \quad K_d\ ]$, where the vector elements correspond to the proportional gain, integral gain, and differential gain of the PID controller, respectively. The population size was specified as 40 and the initial set of candidate solutions was obtained using the QRS method. As described in Section 3, the fitness of the various candidate solutions was evaluated using the IAE performance index. During the iterative solution procedure, new candidate solutions were produced using a Gaussian mutation process. Finally, the optimization procedure was terminated after 300 iterations.

As shown in Fig. 5.3, the IAE metric converged to a final value of 0.3829 in the EP optimization procedure, corresponding to PID gain constants of $[\,K_p \;\; K_i \;\; K_d\,] = [\,14 \;\; 0 \;\; 0.002\,]$. The optimal parameters of the PID controller were then finely tuned using an FLC scheme based on the membership function shown in Fig. 5.4. Note that the fine-tuning process was performed in accordance with

$$\begin{cases} e_1 = R(t) - Y(t) \\ e_2 = \dot{e}_1 \end{cases} \tag{5.1}$$

where e_1 is the error between the input reference value (R) and the system output value (Y) and e_2 is the rate of change of e_1.

Figure 5.5 shows the convergence of the rotational position of the DC servo motor shaft to the instructed position (45°) given the use of the EP-based PID controller and the FLC + EP based PID controller, respectively. It is seen that the convergence time given the use of the EP-determined PID parameter values is equal to 0.156 seconds.However, when the PID parameter values are further tuned using the FLC controller, the convergence time reduces to 0.139 seconds. In other words, the FLC + EP based PID controller reduces the convergence time by around 11%.

The optimal PID parameters were also determined using the GA method. (Note that the algorithm settings were identical to those used in the EP algorithm). The IAE metric was found to converge to a value of 0.39 (see Fig. 5.6)), corresponding to optimal PID gains of $[\ K_p \quad K_i \quad K_d\ ] = [\ 13.982 \quad 0.05 \quad 0.002\ ]$. Figure 5.7 compares the transient responses of the servo motor when controlled by the GA-based PID controller and the FLC+GA based PID controller, respectively. From inspection, the FLC+GA based controller is found to reduce the convergence time from 1.16 seconds to 1.12 seconds.

Finally, Fig. 5.8 compares the transient responses of the servo motor when controlled by the FLC + EP based controller and the FLC + GA based controller, respectively. The results confirm that the FLC + EP controller yields a more rapid transient response than the FLC + GA controller.

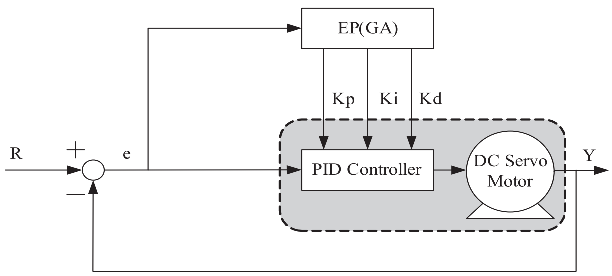

Figure 5.1: EP (GA) based PID control system.

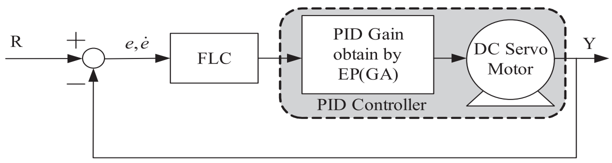

Figure 5.2: FLC+EP (FLC+GA) based PID control

system.

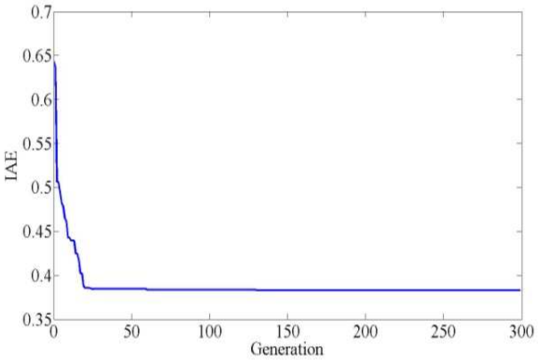

Figure 5.3: IAE convergence curve in EP optimization procedure.

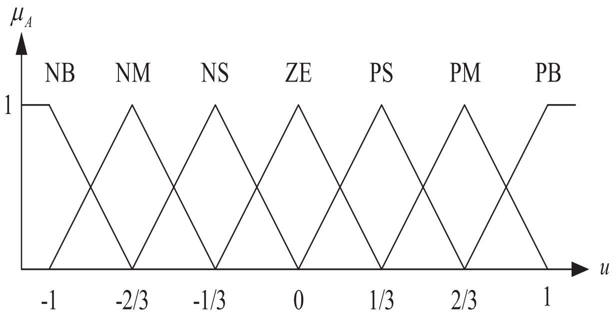

Figure 5.4: Membership function of FLC controller.

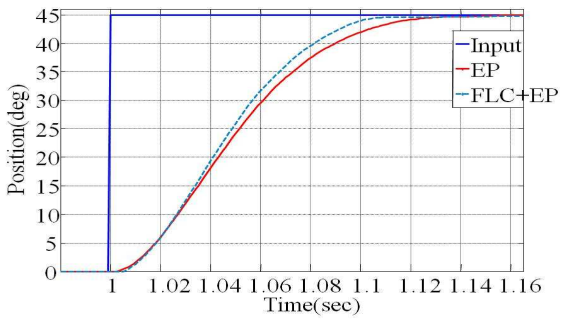

Figure 5.5: Transient response of servo motor under EP and FLC + EP control schemes.

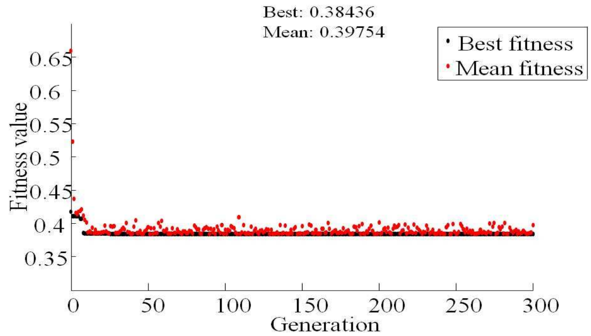

Figure 5.6: IAE convergence curve in GA optimization procedure.

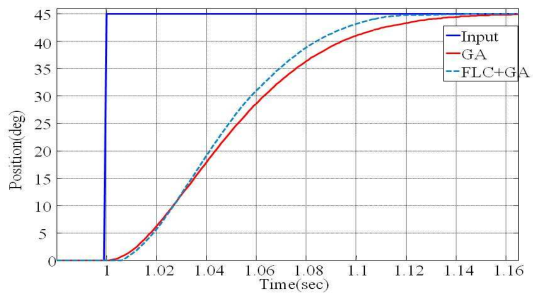

Figure 5.7: Transient response of servo motor under GA and FLC + GA control schemes.

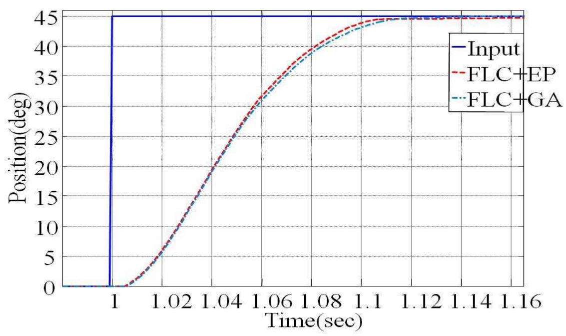

Figure 5.8: Transient response of servo motor under FLC+GA and FLC + GA control schemes.

6 Conclusions

This paper has presented two PID-based control schemes for a DC servo motor. In the first scheme, the optimal gain constants of the PID controller are determined using an EP optimization algorithm, while in the second scheme, the optimal gains are determined using a GA. In both cases, the optimal gains have been fine-tuned using a FLC system. The experimental results obtained using a commercial servo motor (SRV02, Quanser Inc.) have shown that for both control schemes, the use of the FLC controller to fine tune the optimal PID gain constants yields an effective reduction in the response time of the servo motor. Furthermore, it has been shown that of the two schemes, the FLC+EP based controller provides a faster transient response.

Acknowledgements

This financial support provided to this research by the National Science Council of Republic of China under contract 98-2221-E-269-019-MY2 is greatly appreciated.

References

[1] D. B. Fogel, *Evolutionary Computation: Toward a New Philosophy of Machine Intelligence*. IEEE Press, Piscataway, New York, (1999).
[2] M. L Hung., J. S. Lin, J. J. Yan and T. L. Liao Optimal PID control design for synchronization of delayed discrete chaotic system. *Chaos, Solitons and Fractals*, **35**, 781-785 (2008).
[3] H. X. Li, L. Zhang, K. Y. Cai and G. Chen, An Improved Robust Fuzzy-PID Controller With Optimal Fuzzy Reasoning. *IEEE-SMCB*, **35**, 1283-1294 (2005).
[4] C. T. Lin and Lee C. S. George, *Neural Fuzzy Systems:A Neuro-Fuzzy Synergism to Intelligent Systems*. Prentice-Hall, (1996).
[5] A. Sevinc, A Full Adaptive Observer for DC servo Motors. *Turk J Elec Engin*, **11**, 117-130 (2003).
[6] M. Faruk, B. Tamer, B. Kurtulus, E. B. Fatih, Optimization of module, shaft diameter and rolling bearing for spur gear through genetic algorithm, *Expert Systems with Applications*, **37**, 8058-8064 (2010).
[7] Quanser, *SRV02-series Rotary Servo Plant of User Manual*, (2004).

Her-Terng Yau received the B.S. degree from the National Chung Hsing University, Taichung, Taiwan, in 1994. Then, he obtained the M.S. and Ph.D. degrees from the National Cheng Kung University, Tainan, Taiwan, in 1996 and 2000, respectively, all in mechanical engineering. In addition, he is a Professor at the Department of Electrical Engineering, National Chin-Yi University of Technology, Taichung, Taiwan, where he currently teaches in the areas of automatic control and signal analysis. His research interests include robust control, nonlinear system analysis and control, fuzzy control, and nano- and microengineered system.

Po-Hsien Yu is currently a university student in Department of Mechanical and Electro-Mechanical Engineering, National Sun Yat-Sen University, Kaohsiung, Taiwan. His research interests are in the areas of mechanical system analysis and control. He is now a part-time research assistant with Prof. Her-Terng Yau

Yuan-Hung Su received the B.S. degree from the Far-East University, Tainan, Taiwan, in 2008. Then, he also obtained the M.S. degrees from the Far-East University, Tainan, Taiwan, in 2010, all in Electrical engineering. His research interests include intelligent control and fuzzy control